Energies **2010**, *3*, 1895-1913; doi:10.3390/en3121895

OPEN ACCESS

energies

ISSN 1996-1073

www.mdpi.com/journal/energies

Article

Creating a Global Grid of Distributed Fossil Fuel CO_2 Emissions from Nighttime Satellite Imagery

Tilottama Ghosh [1,*], Christopher D. Elvidge [2], Paul C. Sutton [3], Kimberly E. Baugh[1], Daniel Ziskin [1] and Benjamin T. Tuttle [3]

[1] Cooperative Institute for Research in Environmental Sciences, University of Colorado, Boulder, CO 80309, USA; E-Mails: kim.baugh@noaa.gov (K.E.B.); daniel.ziskin@noaa.gov (D.Z.)

[2] Earth Observation Group, Solar and Terrestrial Physics Division, NOAA National Geophysical Data Center, 325 Broadway, Boulder, CO 80305, USA; E-Mail: chris.elvidge@noaa.gov

[3] Department of Geography, University of Denver, Denver, CO 80208, USA; E-Mails: paul.sutton@du.edu (P.C.S.); btuttle@du.edu (B.T.T.)

* Author to whom correspondence should be addressed; E-Mail: tilottama.ghosh@noaa.gov; Tel.: +1-303-497-6385; Fax: +1-303-497-6513.

Received: 21 November 2010; in revised form: 6 December 2010 / Accepted: 7 December 2010 / Published: 8 December 2010

Abstract: The potential use of satellite observed nighttime lights for estimating carbon-dioxide (CO_2) emissions has been demonstrated in several previous studies. However, the procedures for a moderate resolution (1 km^2 grid cells) global map of fossil fuel CO_2 emissions based on nighttime lights are still in the developmental phase. We report on the development of a method for mapping distributed fossil fuel CO_2 emissions (excluding electric power utilities) at 30 arc-seconds or approximately 1 km^2 resolution using nighttime lights data collected by the Defense Meteorological Satellite Program's Operational Linescan System (DMSP-OLS). A regression model, Model 1, was initially developed based on carbon emissions from five sectors of the Vulcan data produced by the Purdue University and a nighttime satellite image of the U.S. The coefficient derived through Model 1 was applied to the global nighttime image but it resulted in underestimation of CO_2 emissions for most of the world's countries, and the states of the U.S. Thus, a second model, Model 2 was developed by allocating the distributed CO_2 emissions (excluding emissions from utilities) using a combination of DMSP-OLS nighttime image and population count data from the U.S. Department of Energy's (DOE) LandScan grid. The CO_2 emissions were distributed in proportion to the brightness of the

DMSP nighttime lights in areas where lighting was detected. In areas with no DMSP detected lighting, the CO_2 emissions were distributed based on population count, with the assumption that people who live in these areas emit half as much CO_2 as people who live in the areas with DMSP detected lighting. The results indicate that the relationship between satellite observed nighttime lights and CO_2 emissions is complex, with differences between sectors and variations in lighting practices between countries. As a result it is not possible to make independent estimates of CO_2 emissions with currently available coarse resolution panchromatic satellite observed nighttime lights. However, the nighttime lights image in conjunction with the population grid can help in more accurate disaggregation of national CO_2 emissions to a moderate resolution spatial grid.

Keywords: CO_2 grid; nighttime satellite image; LandScan population grid

1. Introduction

Since the beginning of the Industrial Revolution, the world's population has continued to increase, adding each subsequent billion in a span of fewer years than ever before. The world hit the 4 billion mark in 1974, 5 billion just 13 years later, in 1987, and passed the 6 billion milestone 12 years later in 1999 [1]. The world population is likely to reach 7 billion in the latter half of 2011, again in a span of 12 years [2]. Population growth has led to land use change through intensification of agriculture, and improved contemporaneous increases in average standards of living have substantially increased energy use [1]. Changing land use and increased fossil fuel combustion for meeting the growing energy demand are the primary causes for augmented carbon dioxide (CO_2) concentration in the atmosphere [3]. The anthropogenic contribution in global warming is substantial and is evident in the rising global and ocean temperatures, extensive melting of snow and ice, and rise in the global average sea level [3]. The need for quantification of anthropogenic fossil fuel CO_2 emissions in the atmosphere at finer spatial and temporal resolutions has been felt by the scientific and policymaking communities since the last decade [4]. From the policy-making perspective it is necessary to construct emission inventories in order to monitor and agree upon emission reduction targets [5]. Spatial distribution of emissions is also an important input to "atmospheric-inversion" methods, which combine CO_2 concentration measurements with transport and process models to estimate land and ocean CO_2 sources and sinks [6–9]. Anthropogenic CO_2 emissions disrupt the equilibrium of the carbon cycle and makes it all the more important to monitor the spatial distribution of CO_2 emissions.

Most of the existing inventory on the spatial distribution of CO_2 emissions is available on a national basis. The U.S. Department of Energy's Carbon Dioxide Information Analysis Center (CDIAC) and the International Energy Agency (IEA) provide a global database of CO_2 emissions for countries. The national geographic distribution of CO_2 emissions has been disaggregated to finer resolutions (1° grid resolution) using population density grids as proxy measures [10–13]. Although the population density grid provides a reasonably good proximate measure of CO_2 emissions at a spatial resolution of 1°, it is not capable of providing satisfactory maps depicting geographic distribution of CO_2 emissions at a resolution finer than this. This is because the population density grids do not depict transportation links

and emissions from power stations. Moreover, the census data on which these population density grids are based are collected at specific spatial units and disaggregating these data to the source regions is problematic [13].

From a satellite remote sensing perspective, it is possible to measure the CO_2 concentration in the atmosphere at coarse spatial resolution using high spectral resolution infrared interferometer data. Examples of such systems include the Japanese Greenhouse Gas Observing Satellite (GOSAT) and NASA's planned Orbiting Carbon Observatory (OCO). With data from these systems the CO_2 signal from major urban centers are diffused and spatially offset from the sources due to the coarse spatial resolution, atmospheric transport, mixing, and retention of CO_2 in the atmosphere. Thus it is difficult to discern increases or decreases in CO_2 emissions from specific cities or towns from systems such as GOSAT by themselves. Application of inversion methods to detect changes in fossil fuel carbon emissions would require surface maps of fossil fuel CO_2 emissions. There are databases that list the locations and estimated emissions for electric power utilities (e.g., Carbon Monitoring for Action "CARMA"). This leaves the spatial distribution of non-point sources (from vehicles, homes and businesses) as a major gap in the mapping of fossil fuel CO_2 emissions that would enable inversion modeling changes in emissions based on GOSAT or OCO style data.

The Defense Meteorological Satellite Program's Operation Linescan System (DMSP-OLS) satellite-observed nightlight data acts as a suitable proximate measure for mapping the distribution of CO_2 emissions at a finer spatial resolution. Elvidge *et al.* [14] was the first to identify the correlation between lit area of lights and CO_2 emissions. Doll *et al.* [15] built upon this relationship and created the first global grid of CO_2 emissions at $1° \times 1°$ resolution. A 6-month 1-kilometer stable light composite acquired between October 1994 and March 1995 was used in this study. Country level relationships between lit area and CO_2 emissions were used to create global maps of these parameters. This map was then compared to CDIAC's CO_2 emissions map. Comparison with CDIAC's CO_2 emissions map showed that the emissions map created from the nighttime lights resulted in an underestimation of CO_2 emissions for most countries. However, the nighttime lights image did a superior job in mapping the spatial distribution of the emissions [16]. Under- and over-estimation of CO_2 emissions predicted from the nighttime image is expected because countries usually have more or less emissions than what is predicted from the nighttime lights, as the lights and CO_2 emissions do not always have a direct linear relationship. This was observed in the case of many of the former Soviet Republics by Doll *et al.* [15]. The authors noted that many of the former Soviet Republics appeared to have more emissions than what was predicted from the nighttime lights [16].

Other recent efforts at developing a fine resolution CO_2 emissions map is the one by Rayner *et al.* [17].They developed a "model-data synthesis" approach called the "Fossil Fuel Data Assimilation System" (FFDAS). Using two main datasets—the gridded population data and satellite observed nighttime lights they produced global fossil fuel CO_2 emission fields based on the Kaya identity. Realizing the saturation of the nighttime lights as a major problem in areas of high light intensity, they developed a "global correction factor" which was used to correct the saturation errors in the nighttime lights image. Then, these 'corrected' spatial data were used to create the fine resolution CO_2 emissions map.

Oda and Maksyutov [13] have developed a global high resolution annual CO_2 emission inventory for the years 1980–2007, named Open-source Data Inventory of Anthropogenic CO_2 emission

(ODIAC) to inform the observational data collected by satellites such as the Japanese Greenhouse gas Observing SATellite (GOSAT), especially for CO_2 emissions regional flux inversions study. They estimated national emissions using global energy consumption statistics. Emissions from power plants were estimated separately using the Carbon Monitoring for Action (CARMA) database. The CARMA CO_2 emissions were directly mapped on power plant locations using the coordinate information, and the residual emissions (total emissions minus power generation emission) were distributed using the nighttime lights image as a proxy. Since the nighttime image is available in 30 arc-second grid (approximately 1 km), the CO_2 emission map was also mapped at a resolution of 1 km^2. In order to correct for the saturation of lights in the city centers in the stable light images, Oda and Maksyutov [13] obtained radiance values from the 1996–1997 radiance-calibrated nighttime image, and using a conversion equation converted the digital number (DN) values between 0–254 for all the stable light images of the years 1980–2007 to radiance values. Oda and Maksyutov [13] determined the spatial distribution of emissions based on a linear correlation between nightlights and CO_2 emissions, and also assumed it to be uniform over different countries, though in actuality the relationship maybe strongly country-dependent. They have discussed these drawbacks in their paper.

Gurney *et al.* [18] at Purdue University have created a Vulcan U.S. fossil fuel CO_2 emissions inventory for the year 2002. The total carbon emissions grid is available in 10 km as well as 0.1 degree resolution and the sectoral carbon emissions are available at 0.1 degree resolution. The Vulcan dataset was developed based on fine scale reported inventory by individual source economic sectors, and is perhaps the best available carbon emissions inventory available for the U.S. at such a fine spatial and temporal resolution. The Vulcan dataset will be discussed in greater details in a later section.

In this paper, we have built upon the previous efforts at creating a global CO_2 emissions grid from the nighttime satellite image and population grid and have tried to address some of the drawbacks of the previous studies. Two separate models were built, Model 1 and Model 2. Model 1 was developed based solely on the statistical correlation between the nighttime lights and selected Vulcan sectors. The coefficient derived from Model 1 was applied to the nighttime lights of the world to estimate global CO_2 emissions. Since the Vulcan emissions data for the U.S. is the best available fine resolution data for any country of the world, it was hypothesized that the coefficients derived through Model 1 when applied to the global nighttime image would provide fairly accurate estimations of CO_2 emissions for other countries as well. However, Model 1 did not provide satisfactory results and so Model 2 was developed. In Model 2, CO_2 emissions were allocated using a combination of DMSP nighttime lights and DOE Landscan population count data.

2. Data Sources

2.1. Nighttime Lights Imagery

In Model 1, the DMSP-OLS nighttime image of 2000 was used to calculate the light intensity values for all the lit areas of the U.S. corresponding to the surface grid extent of the Vulcan dataset. For Model 2, the DMSP-OLS nighttime image was used to compute the sum of light intensity values of all the administrative units, demarcate the population in the lit and dark areas of the world, and to distribute the estimated CO_2 emissions from the lit areas. A merged stable lights and radiance-calibrated image of 2000 was used in this study (Figure 1). The National Geophysical Data Center (NGDC) of

the National Oceanic and Atmospheric Administration (NOAA) has been archiving and processing Defense Meteorological Satellite Program's Operational Linescan System (DMSP-OLS) nighttime lights data since 1994. The stable lights data of 2000 were composited from hundreds of cloud-free orbits for the year 2000, with the ephemeral light sources, such as fires and lightning removed [19]. The stable lights data suffer from saturation of light intensity values in the brightly lit city centers. The radiance-calibrated images, on the other hand, are produced by combining images collected at different gain settings (high, medium, and low), and thus can help to deal with the problem of saturation of city centers and also provide a much better view of the internal structure of cities [20]. Merging the stable lights and radiance-calibrated image of 2000 therefore makes it possible to include the best features of both types of nighttime lights dataset. For this study, the lights produced by gas flaring activities were masked out. CO_2 emissions from gas flares are excluded from national emissions reporting based on fossil fuel consumption. The gas flares were masked out of the nighttime lights based on the delineations developed by Elvidge *et al.* [21].

Figure 1. Merged stable lights and radiance-calibrated DMSP-OLS nighttime image of 2000.

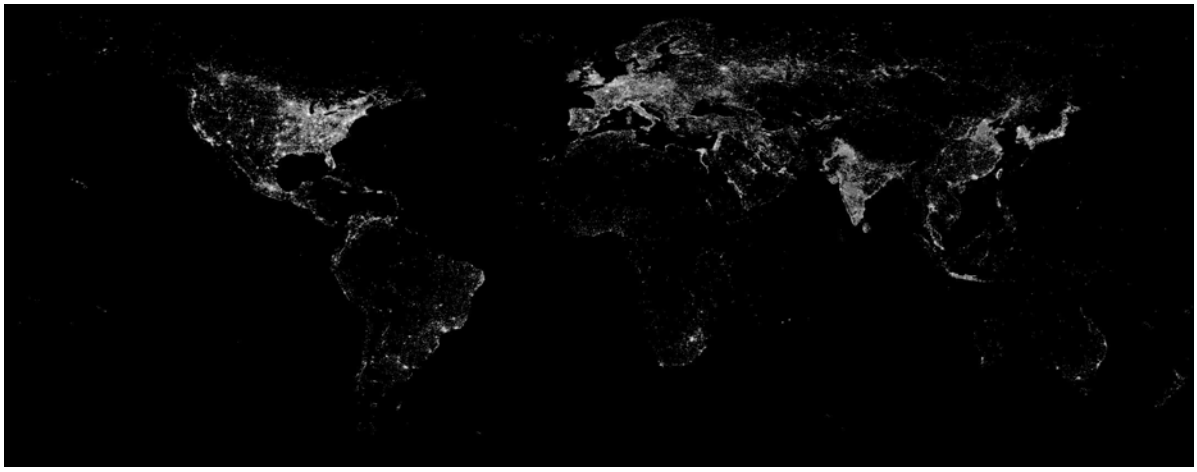

The spatial resolution of the smoothed nighttime lights data is 2.7 km. However, the images are geolocated to 30 arc-second grids, which is approximately 1 km^2 at the equator. The latitudinal extent of the image is from 75°N to 65°S and the longitudinal extent is from 180°W to 180°E.

2.2. LandScan Population Grid

The LandScan population grid of 2000 was used in Model 2 to derive the total population in the lit and dark areas of the administrative units and also to distribute the estimated CO_2 emission values in the dark areas of the world where there are settlements but no lights (Figure 2). The LandScan population dataset is a progressive series of spatially disaggregated global population count datasets that is produced by the Department of Energy at Oak Ridge National Laboratory. The LandScan model uses spatial data and image analysis techniques, in conjunction with a multi-variable dasymetric modeling approach, to allocate sub-national level census counts to each grid cell based on proximity to roads, slope, land cover, and other information within an administrative boundary. The cells represent ambient population counts in integer values. Ambient population takes into account the movement of people for work or travel and not only where people sleep. The dataset has a spatial resolution of

30 arc-seconds [22]. In order to match the geographic extent of the nighttime image, the LandScan population grid was cropped to 75°N (originally extends to 84°N) and the southern latitudinal extent was cropped to 65°S (originally extends to 90°S).

Figure 2. LandScan population grid of 2000.

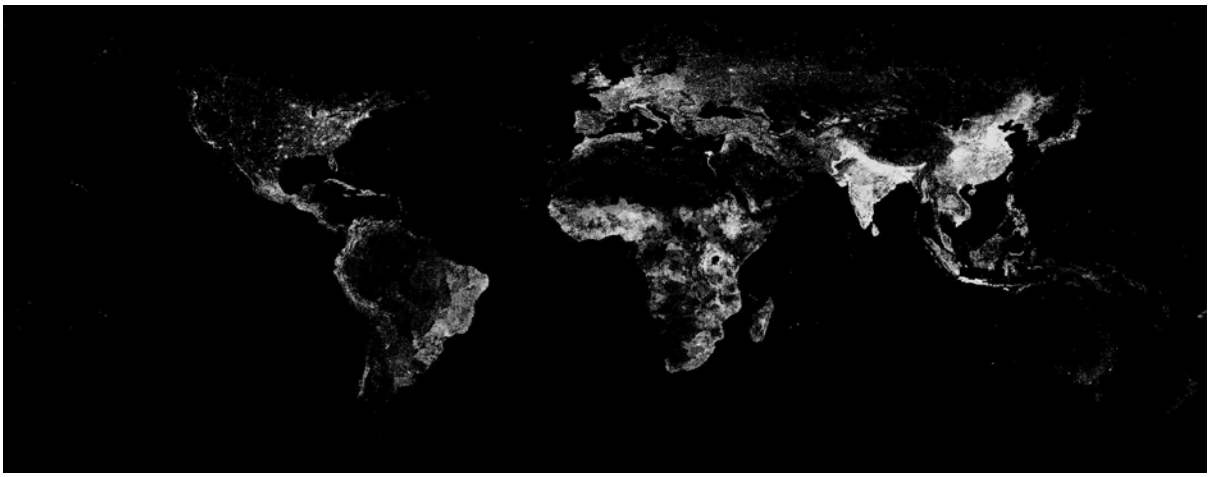

2.3. Vulcan Data

The Vulcan fossil fuel carbon emission inventory provides a unique spatial depiction of the carbon emissions for key functional sectors. The currently available Vulcan dataset is for the year 2002. It was produced at Purdue University along with other collaborators at Colorado State University and Lawrence Berkeley National Laboratory [18] and was based primarily on emission inventories. The data cover the continental U.S. at a spatial resolution of 0.1° × 0.1°, reporting carbon emissions in units of tonnes of carbon/hour/gridcell. The longitudinal direction has 650 gridcells, and the latitudinal direction has 280 gridcells and the time dimension has 8,760 timesteps. Inputs include carbon emission inventory data from the Environmental Protection Agency (EPA), National Emission Inventory (NEI) and other data on mobile sources, power plants, and U.S. census data. All emitting locations are geocoded to latitude, longitude, and postal address. Emissions from fixed locations are divided among residential, commercial, industrial, utilities and cement production sectors. The transport sector contains three separate components: on road or mobile sector emissions (mobile transport using designated roadways), non-road emissions (e.g., boats, trains, all terrain vehicles (ATVs), and emissions associated with air travel (airports and airborne craft)) (Figures 3).

2.4. Reported Carbon-Dioxide (CO_2) Emissions Data—Countries of the World and States of the U.S.

Reported total CO_2 emissions data, for the year 2000, for all the countries of the world were retrieved from United Nations Millennium Indicators website [23] although the primary data source is the Carbon Dioxide Information Analysis Center (CDIAC). CDIAC housed in the Department of Energy's (DOE) Oak Ridge National Laboratory is one of the primary sources of climate change data. CO_2 emissions data in thousand metric tonnes for 206 countries were procured from CDIAC's data repository. Data on CO_2 emissions for only two countries, Liechtenstein and Monaco, were taken from

United Nations Framework Convention on Climate Change (UNFCCC) as emission values for these two countries were not available from CDIAC's data repository [23].

Figure 3. Vulcan sectoral carbon emissions data, 2002. Note that a contrast enhancement was applied to each image to reveal the spatial features.

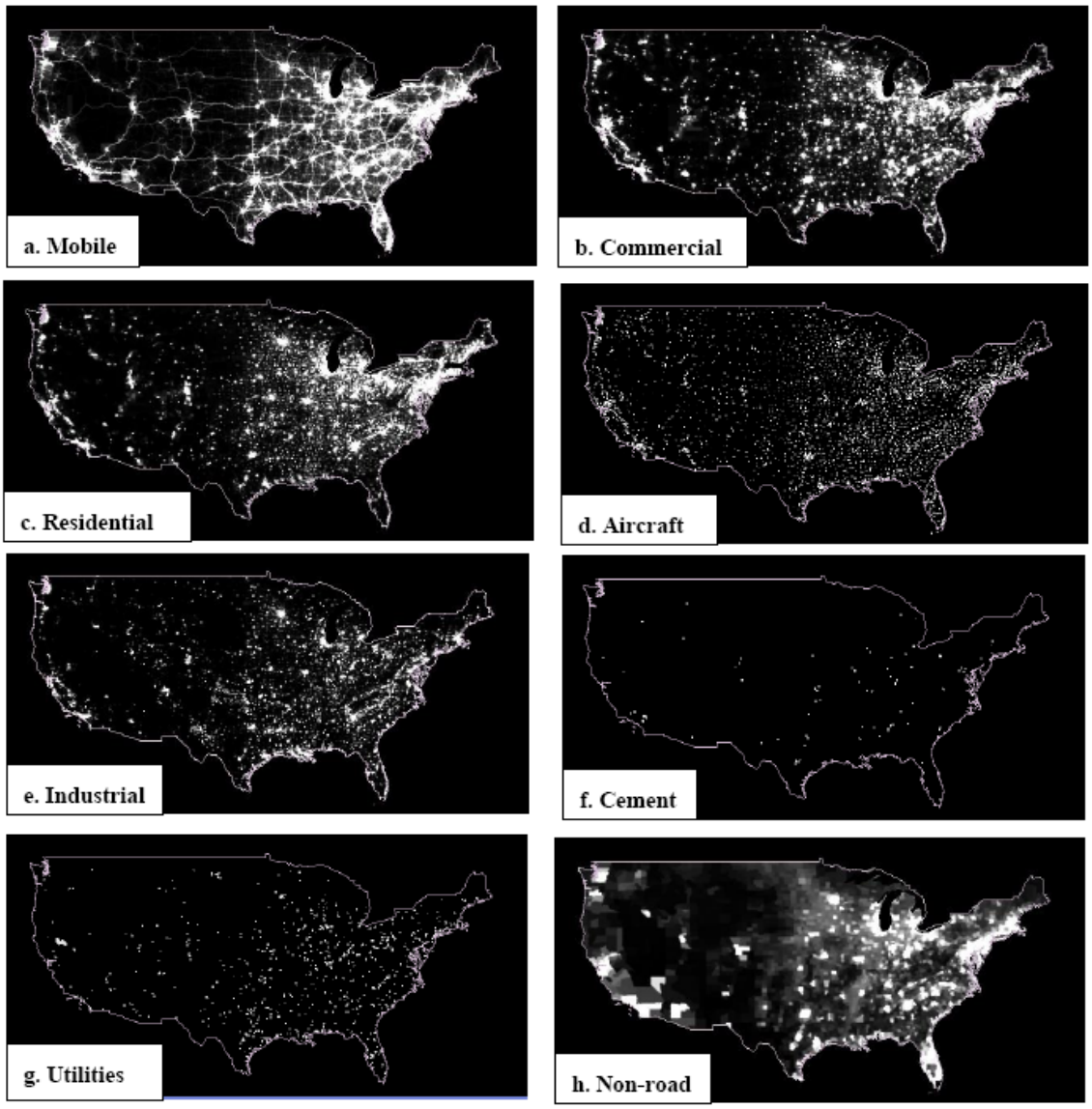

The total CO_2 emissions data for the states of the U.S. were available from the U.S. Environmental Protection Agency's (EPA) website. The EPA provides state CO_2 emission inventories from fossil fuel combustion, by end-use sector (commercial, industrial, residential, transportation, and electric power), in million metric tonnes of carbon dioxide from 1990 through 2007 [24]. We used the data of 2000 for our analysis.

The reported CO_2 emissions with the electric power plant emissions subtracted from them (Figure 4) were used to compare the estimated CO_2 emissions derived through multiplying the nighttime lights grid with the coefficient derived through Model 1, and in Model 2 the non-utility CO_2 emissions were distributed using the nighttime lights grid and the LandScan population grid.

Figure 4. Reported non-utility CO_2 emissions data in thousand tonnes, 2000.

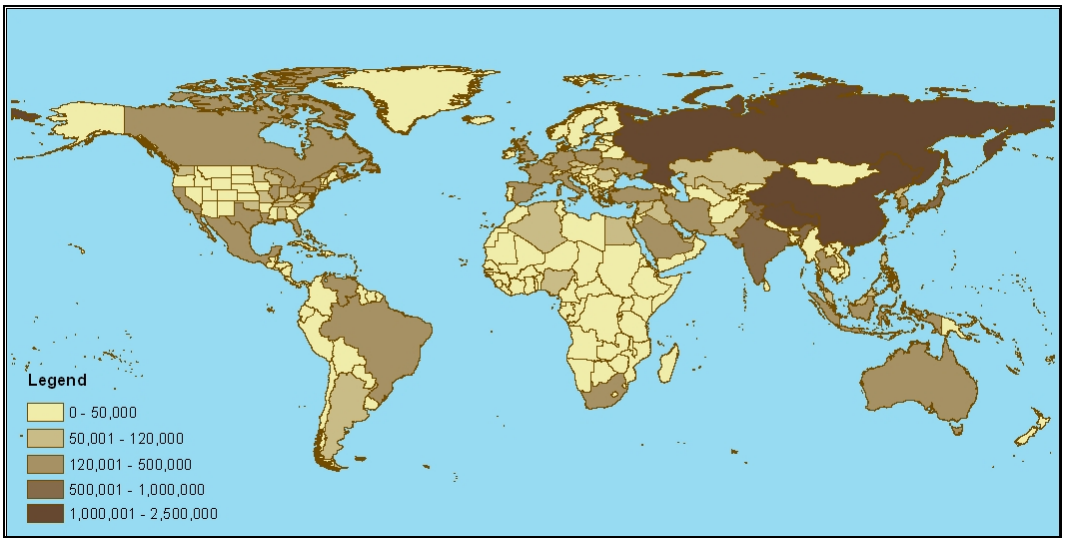

2.5. Carbon-Dioxide (CO_2) Emissions Data from Electric Power Plants—Countries of the World and States of the U.S.

The nighttime lights satellite images can account for the distribution of the CO_2 emissions but cannot fully articulate intense emission from major point sources, such as power plants [13]. Therefore, power plant CO_2 emissions data were subtracted from reported total CO_2 emissions data for all administrative units. Power plant emissions data for all countries of the world were obtained from the Carbon Monitoring for Action (CARMA), which is a huge database including information on the carbon emissions of over 50,000 power plants and 4,000 power companies worldwide. The CARMA power plant CO_2 emissions data of all countries were compared with the data obtained from the World Resources Institute and they were 99% correlated [25]. The data for all the available countries were downloaded. The data were in 'short' or 'U.S. tons', and were converted to metric tonnes by multiplying the values with the conversion factor of 0.90718474.

CO_2 emissions from electric power plants for the states of the U.S. which were derived from EPA are the point source emissions. These emission values were subtracted from the total CO_2 emissions (sum of commercial, industrial, residential, transportation) for the states of the U.S.

3. Methods and Results

The estimated CO_2 emissions grid of the world which was created from the DMSP-OLS nighttime lights image and the LandScan population grid were developed through experimentation with two models. Model 1, based solely on the correlation between the nighttime lights and the Vulcan dataset did not give satisfactory results, and so Model 2 was developed. The two models are discussed separately.

3.1. Model 1

Visual comparison of the Vulcan sector images indicates that several of the sectors are correlated to nighttime lights. To investigate this further we used a stepwise linear regression to determine the best

combination of Vulcan sectors for estimating the brightness of the DMSP nighttime lights. The basis of this development is that the DMSP sensor measures lighting across multiple sectors, with lights detected in residential areas, along streets and roads, in commercial centers, at airports and in industrial areas. To develop this model we first aggregated the nighttime lights to match the spatial resolution of the Vulcan data. A stepwise regression using the JMP statistical software indicated that the carbon emissions from the five sectors - mobile, commercial, residential, industrial, and aircraft sectors, which together account for about 57% of total carbon emissions in the continental U.S., also provide the best model and the highest coefficient of determination ($R^2 = 0.67$) when regressed against the nighttime lights of the U.S. (Table 1). Inclusion of any or all of the remaining three sectors (utilities, non-road, and cement) in the subsequent models of the stepwise regression had a negligible effect on the correlation. The five sectors which together provide the highest R^2 with the lights of the U.S. in the stepwise regression model were added up (Figures 5a,b) and a regression model (Model 1, Figure 6) was developed to derive the coefficient, which was applied on a global basis. For this regression model the intercept was taken as zero implying that carbon emissions are zero when the light intensity value is zero.

Figure 5. (**a**) Vulcan mobile, commercial, residential, aircraft, and industrial sectors added together; (**b**) DMSP-OLS Nighttime lights of the U.S., 2000.

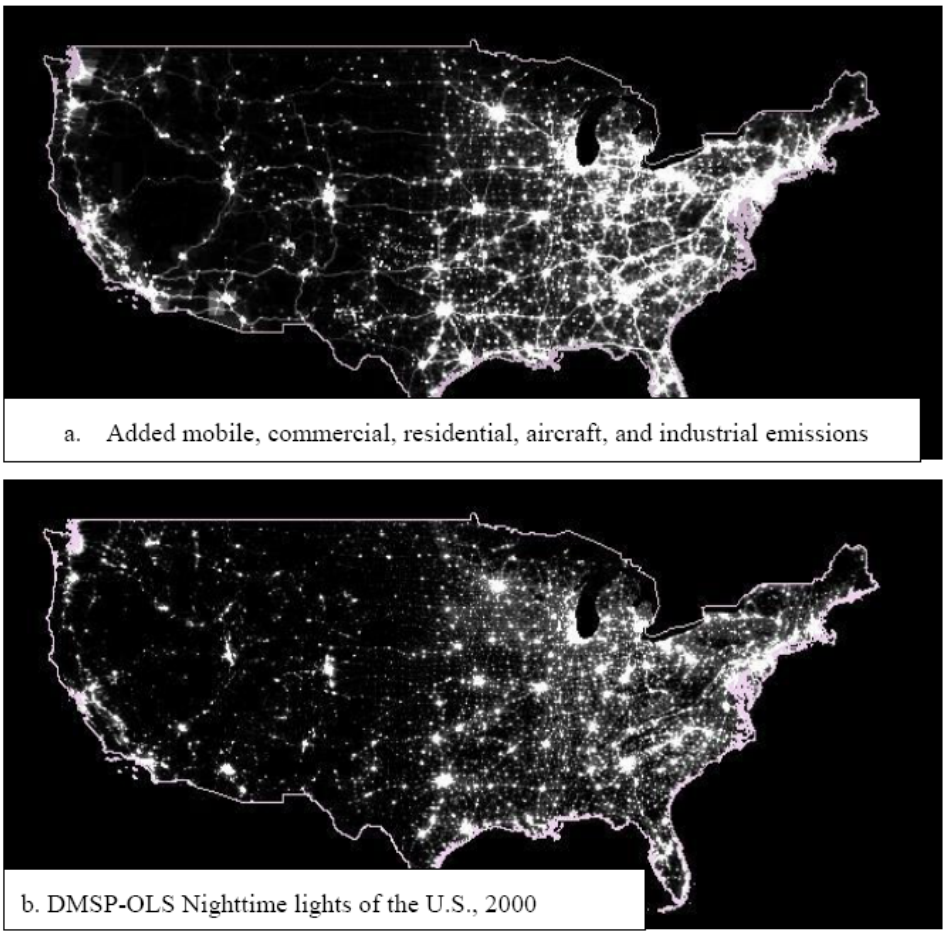

a. Added mobile, commercial, residential, aircraft, and industrial emissions

b. DMSP-OLS Nighttime lights of the U.S., 2000

The coefficient derived through Model 1 (β_{1US}) was multiplied with the light intensity value in each pixel of the nighttime lights image of continental U.S., to derive the modeled carbon emissions grid of

the U.S. At this point we were interested to evaluate the goodness of fit of the nighttime lights emission model vis-a-vis the five individual Vulcan sectors (mobile, residential, commercial, aircraft, industrial). An outlier image for each of the five sectors was calculated by subtracting the nighttime lights based emissions grid from the Vulcan carbon emissions grid of each of the five sectors separately, retaining only the positive values. Examination of these outlier images indicated that the nighttime lights based model was systematically underestimating the CO_2 emissions in several of the sectors. To develop a metric for this underestimation we divided the sum of the outliers in each of the sector by the total carbon emissions of each of the sectors and calculated a percentage underestimation. The underestimation was highest for the mobile and industrial sectors (Table 1).

Figure 6. Model 1—The regression model of the nighttime lights of the U.S. and the Vulcan carbon emissions data of the five sectors (mobile, commercial, residential, aircraft, and industrial sectors) combined.

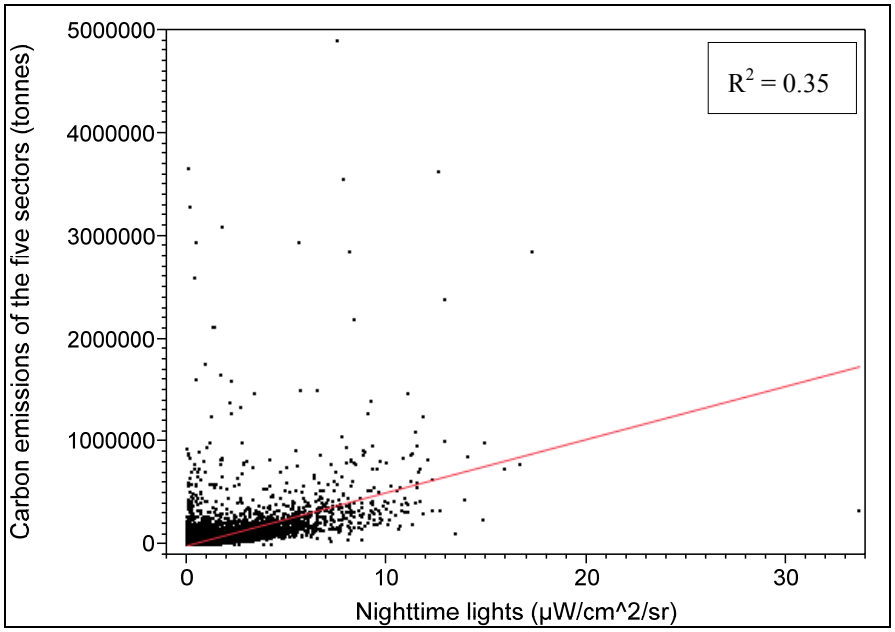

$CO_{2p}' = \beta_{1US} * L_p$, (1)

where, CO_{2p}' = Estimated CO_2 emission for each pixel p

L_p = Light intensity value for each pixel p in the nighttime lights image

β_{1US} = slope coefficient derived through Model 1 (Value of $\beta_{1\,US} = 51678$)

The coefficient derived through Model 1 (β_{1US}) was also multiplied with the light intensity value of each pixel (L_p) in the global nighttime lights grid and the value of 3.67 (ratio of the molecular weight of CO_2 (44) to the atomic weight of carbon (12) = 44/12 = 3.67, as the Vulcan data is provided in terms of the mass of carbon atom) to get the estimated CO_2 emission values for each 1 km^2 pixel in the nighttime lights grid (CO_{2p}') (Equation1). The estimated CO_2 emissions were then aggregated to the administrative units, CO_{2i}', where "i" corresponds to each administrative unit.

The CO_2 emissions from electric power utilities reported by CARMA and EPA were subtracted from the reported CO_2 emission values obtained from CDIAC and UNFCCC for the countries, and EPA for the states of the U.S. Plotting the aggregated estimated CO_2 emissions of the administrative units (CO_{2i}') against the non-utility reported CO_2 emission values (CO_{2i}), provided a correlation

coefficient of 0.86. However, the CO_2 emissions were underestimated for most of the administrative units, except for a few (Figure 7).

Table 1. Coefficient of determination derived from the stepwise regression, percentage contribution of each sector to the total carbon emissions, and the underestimation percentages of each of the five Model 1 sectors.

Vulcan sectoral carbon emission	R^2	% Contribution of each sector to the total carbon emissions	% Underestimation
Mobile	0.6433	27.94	20.43
Non-road	0.3724	3.14	
Residential	0.3628	6.36	2.62
Commercial	0.3116	4.12	7.38
Aircraft	0.1398	1.19	6.25
Industrial	0.0555	17.56	37.24
Utilities	0.0130	38.81	
Cement	0.0011	0.87	
Aircraft, Mobile, Residential, Commercial, Industrial (in the stepwise regression)	0.6708	57.17	

Figure 7. Reported non-utility CO_2 emission values versus modeled (Model 1) CO_2 emission values for the countries of the world and the states of the U.S.

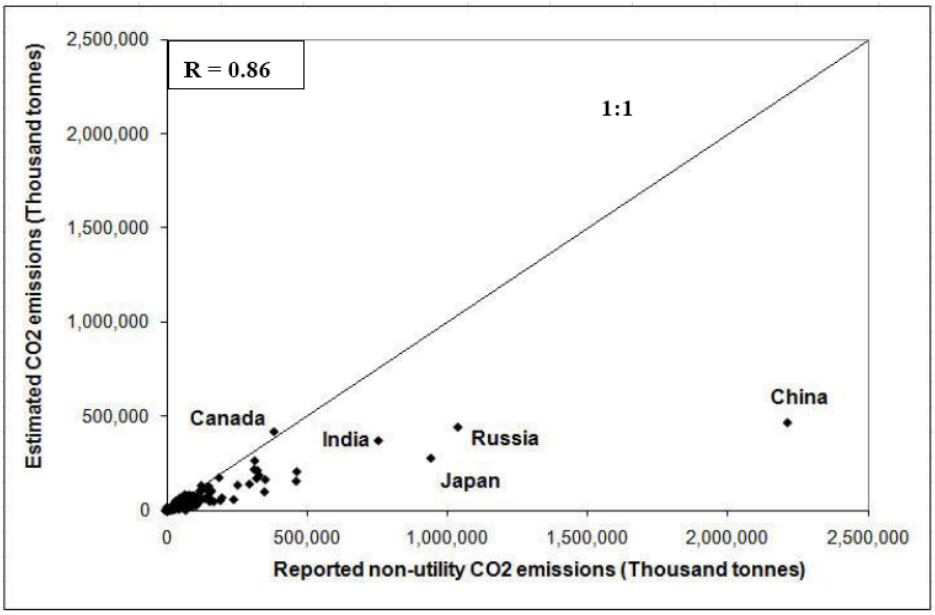

3.2. Model 2

A single coefficient derived from the U.S. Model 1 resulted in underestimation of CO_2 emissions for most of the countries and even most states in the U.S. We attribute this to variations in CO_2 emissions that are independent of the quantity of light emitted to the sky and variations in lighting use patterns between countries. Similar results were alluded to in previous studies [13,15]. Moreover,

regressing the sum of lights against the reported CO_2 emission values of the administrative units (Figure 8) show that countries such as Canada are brighter compared to their CO_2 emission values, whereas, countries such as China have higher CO_2 emission than what is estimated from the nighttime light intensity values.

Figure 8. Regression relationship between sum of lights and reported non-utility CO_2 emissions for all countries and states of the U.S.

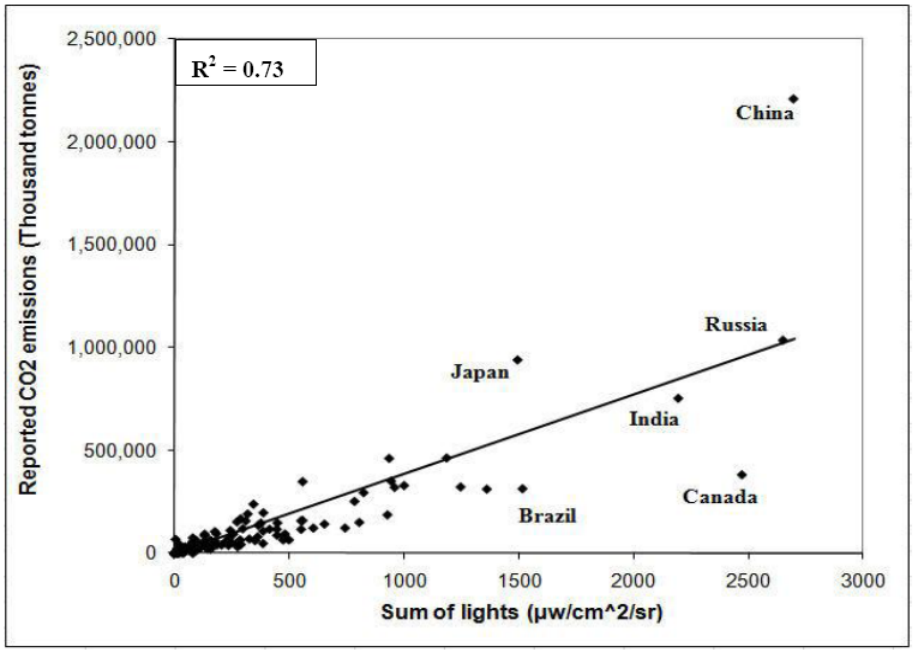

Furthermore, although the nighttime lights can identify the locations for the CO_2 emissions from the lit areas of the world, there are more than 1.6 billion people living in areas with no DMSP light detections [26].

As a result of these considerations, we began the development of a Model 2, which performs a spatial allocation of the reported CO_2 emissions (minus the emissions from electric power utilities) based on nighttime lights and population count. An attempt was made to use lights and population count together; however this regression yielded a negative slope for population and negative CO_2 emissions for many grid cells. To resolve this problem we developed a model which estimated CO_2 emissions in lit areas based on the DMSP nighttime lights and the CO_2 emissions in areas without DMSP lights based on population count. We proceeded with the assumption that people living in areas with no detected DMSP lighting have half the CO_2 emissions as people living in the lit areas of an individual country.

In actuality, the CO_2 emissions per capita from the rural areas (corresponding to the darker areas of the nighttime lights image) vary from one country to another. For example, CO_2 emissions per capita in the U.S. are higher in rural (non-illuminated) areas [27], whereas, CO_2 emissions per capita in India are lower in rural areas. Again, for the quarter of the world's population in darkness, the percentage varies between countries. In a recent paper estimating the electrification rates of countries using the nighttime satellite image [26] it was estimated that only about 1% of the U.S. population is in darkness, whereas about 25% of the population is in darkness in China and India. Thus, the factor with

which the nighttime lights pixel should be multiplied to get the CO_2 emissions per capita from the non-illuminated rural areas is a variable. In the absence of a better known number the 0.5 factor was used as a placeholder for demonstrating the CO_2 production of non-illuminated areas. Ultimately it would be ideal to produce a map of this parameter that varies from country to country. Future research will undoubtedly improve the characterization of this parameter.

At first a mask of the lit areas of the world was created from the nighttime lights grid. This mask was overlaid on the LandScan population grid and the sum of population of the lit areas of each administrative unit was extracted (SOP_{Li}). Similarly, a mask of the dark areas of the world was created from the nighttime image and was overlaid on the population grid to extract sum of population of the dark areas of each administrative unit (SOP_{Di}). The reported non-utility CO_2 emissions of the administrative units (CO_{2i}) were distributed between the dark and lit areas based on the following equation (Equation 2).

$$CO_{2i} = CO_{2Li} + CO_{2Di} \quad (2)$$

$$CO_{2i} = (SOP_{Li} * x_i) + (SOP_{Di} * x_i/2)$$

$$x_i = CO_{2i}/(SOP_{Li} + SOP_{Di}/2)$$

Through Equation 2 the value of the variable "x_i" for each administrative unit was derived. The variable x_i was then multiplied with the sum of population in lit areas for each administrative unit i (SOP_{Li}) and half of the variable x_i, that is, $x_i/2$, was multiplied with the sum of population in the dark areas for each administrative unit i (SOP_{Di}). This provided the total CO_2 emissions from the lit areas (CO_{2Li}) and total CO_2 emissions from the dark areas (CO_{2Di}), respectively, for each administrative unit. (Equations 3 and 4).

$$CO_{2Li} = SOP_{Li} * x_i \quad (3) \qquad CO_{2Di} = SOP_{Di} * (x_i/2) \quad (4)$$

The CO_2 emissions from the lit areas (CO_{2Li}) were then divided by the sum of lights (in radiance units) for each administrative unit (SOL_{Li}). This yielded the CO_2 emissions per radiance unit for each administrative unit. Conversely, CO_2 emissions from the dark areas (CO_{2Di}) were divided by sum of population in the dark areas (SOP_{Di}) to get CO_2 emissions per person for the dark areas for each administrative unit. In order to distribute the CO_2 emissions from the lit areas, each of the lit pixels of the nighttime lights grid (L_p) was multiplied by the CO_2 emissions per radiance unit for that administrative unit (Equation 5). Conversely, to distribute the CO_2 emissions from the dark areas the population count in each pixel of the dark areas of the population grid (P_{Dp}) were multiplied by the CO_2 emissions per person for the dark areas for that administrative unit (Equations 6).

$$CO_{2Lp}' = (CO_{2Li}/SOL_{Li})* L_p \quad (5) \qquad CO_{2Dp}' = (CO_{2Di}/SOP_{Di})* P_{Dp} \quad (6)$$

These two separate CO_2 emissions grid from the lit areas and the dark areas of the world (CO_{2Lp}' and CO_{2Dp}') were added to create the final estimated CO_2 emissions grid (CO_{2p}') (Equation 7, Figure 9a).

$$CO_{2p}' = CO_{2Lp}' + CO_{2Dp}' \quad (7)$$

The disaggregated CO_2 emissions map represents values in tonnes assigned to 1 km^2 pixels, or CO_2 emissions in tonnes/km^2/year. In the disaggregated map the ocean pixels have a value of 0. Also,

pixels in the inaccessible areas of the world, such as the high mountainous areas and deserts, with no population or nighttime lights also have a value of 0. The major cities and urban areas of the world have CO_2 emissions greater than 500 tonnes/km^2/year. Areas of the world which have population but no lights have CO_2 emissions less than 50 tonnes/km^2/year. Figure 9(a) shows the CO_2 emissions grid of the world, and Figures 9(b), (c), (d), and (e) show CO_2 emissions of North-eastern United States, Japan, Eastern China, and Northern India, respectively.

Figure 9. Estimated CO_2 emissions grid in tonnes/km^2/year.

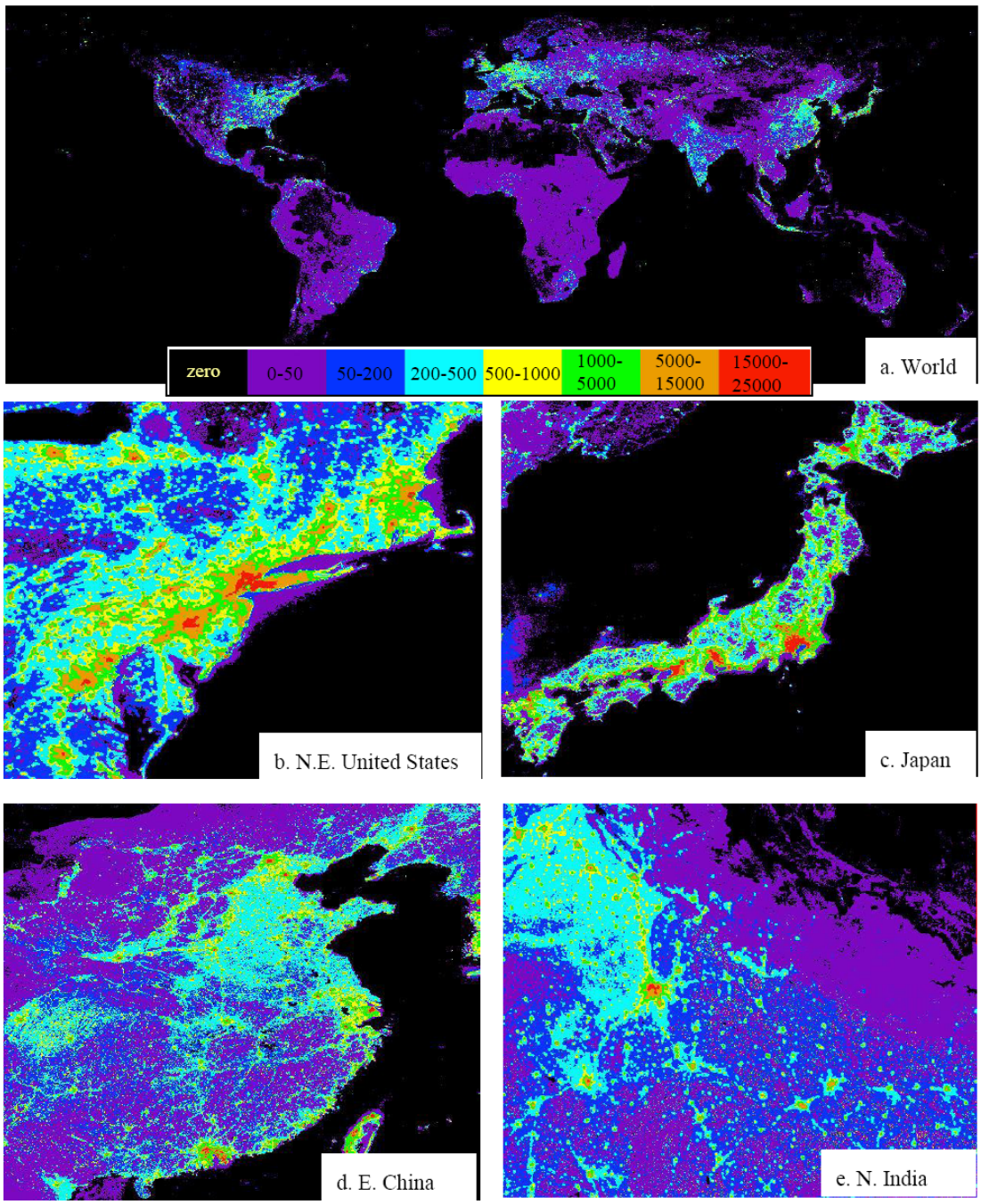

In order to check how well Method 2 worked in creating the disaggregated map of CO_2 emissions, we aggregated the emissions in each pixel (CO_{2p}') to the level of the administrative units (CO_{2i}') and compared it to the reported non-utility CO_2 emission values (CO_{2i}). The relation between the estimated

and reported non-utility CO_2 emissions at the level of the administrative units provided a correlation of coefficient of 1, implying perfect correlation between the reported and estimated variables.

5. Discussion and Conclusion

Two separate models were built for creating a disaggregated map of global non-utility CO_2 emissions. The first model was based on a regression relationship between the nighttime lights of the U.S. and the combined carbon emissions of the five sectors (residential, commercial, aircraft, industrial, and mobile sector) of the Vulcan data. The slope coefficient derived through this relationship (CO_2 emissions per radiance) was multiplied with the global nighttime lights radiance data and this provided the estimated CO_2 emissions grid. However, when this estimated CO_2 emissions grid was aggregated to the level of the administrative units it was seen that CO_2 emissions were underestimated for almost all administrative units. Thus, it was realized that a single coefficient derived through a regression relationship developed for the U.S would not enable accurate estimations of CO_2 emissions for all administrative units. Based on the Vulcan data we found the underestimation to be highest (Table 1) in the industrial and mobile (streets, roads and highways) sectors. We attribute this underestimation in part to the inability of a single coefficient to adequately represent the differences that exist between carbon emissions across multiple sectors. For instance, on a per square kilometer basis the CO_2 emissions from residential areas is undoubtedly lower than the emissions from a heavily trafficked highway of an industrial facility. Another aspect of the underestimation is that Model 1 assumes that the use of lighting in each country is comparable to the U.S. The vast underestimation of CO_2 emissions in China under Model 1 suggests that China uses far less lighting per person than the U.S. Previous studies [19,26] have indicated that there are variations in lighting types, lighting fixtures, and lighting preferences that affect the brightness of satellite observed nighttime lights. In order to address these drawbacks Model 2 was developed.

To address these shortcomings with the available data sources we developed Model 2, which uses nighttime lights grid and the LandScan population grid to model the spatial distribution of reported CO_2 emissions (minus those associated with electric power utilities). The use of LandScan population grid in estimating CO_2 emissions proved to be advantageous because population count can serve as a proxy for estimating CO_2 emissions in areas in the world which have no satellite detected lighting. Furthermore, since in the LandScan population model, sub-national level census accounts are allocated to each grid cell based on proximity to roads, slope, and land cover; transportation links are depicted in greater details in the LandScan population grid. Thus, inclusion of the LandScan population grid in the model for estimating CO_2 emissions ensured the estimation of emissions from the transport linkages. These road linkages contributed to the outlier percentages from the Vulcan mobile sector emissions when the modeled carbon emissions grid of the U.S was created from its nighttime lights. Model 2 was developed with the assumption that per capita CO_2 emissions from the dark areas of the world were one-half of the per capita emission in the lit areas. On the basis of this assumption, the total reported non-utility CO_2 emissions were distributed into the lit and the dark areas of the world using the nighttime lights image and the LandScan population grid. In Model 2 the total CO_2 emissions are constrained to match the reported values minus the component associated with electric power utilities.

It is important to note that DMSP nighttime lights indicate the spatial distribution for the majority of CO_2 emissions but that they cannot articulate the variability that exists between sectors. If the CO_2 estimation coefficient is tuned to work well for residential and commercial sectors, the emissions for industrial and mobile will be underestimated. With higher spatial resolution and multispectral nighttime lights it would be possible to distinguish the lighting from residential, commercial/industrial, and transportation sectors [28,29]. While such a Nightsat sensor has not been built, the prospects for making improved CO_2 emission grids with such data are clear. It may even be possible to estimate the CO_2 emissions from electric power utilities with Nightsat data. Electric power utility emissions accounts for 40% of all carbon emissions in the United States and about one-quarter of global emissions [25]. Thus, by excluding the utility emissions, the CO_2 emissions grid created from the nighttime lights image and population grid actually maps the distribution of about 75% of all distributed CO_2 emissions.

The method developed here is not an independent method for estimating CO_2 as reported CO_2 emission values were used to set the coefficients for the spatial allocation performed in each administrative unit. However, it is an easy and quick method for estimating and mapping CO_2 emissions at a fine spatial resolution. Moreover, the availability of radiance-calibrated nighttime lights image has made it possible to map variability in distribution of CO_2 emissions into bright urban cores, where previous nighttime lights products contained saturated data values. The NGDC at NOAA is currently producing a radiance-calibrated time series for the years 1996–97, 1999, 2000, 2003, 2004, and 2010. The method developed in this paper could be used to create disaggregate maps of CO_2 emissions for all of these years. However, it should be noted that the lack of on-board calibration for the DMSP nighttime visible band complicates the direct comparison of the data values across the time series.

The greatest advantage of creating a disaggregated map of CO_2 emissions is that it can be aggregated to different environmental, physical, and socio-economic units of analysis and can be easily integrated with other physical and environmental data available in gridded format. Such a fine resolution disaggregated map of CO_2 emissions would also aid in CO_2 emissions regional flux inversions studies. These model outputs can also inform the monitoring of the progress of countries as they move towards achieving emission reduction targets.

Although not an entirely flawless method, the second model developed in this paper provides a simple, useful, and inexpensive technique to create a fine resolution CO_2 grid of the entire planet. Model 2 was developed entirely as a proof of concept. With the availability of better CO_2 emissions data from the dark as well as the lit areas of the world we hope to refine the method and create better fine resolution CO_2 emissions grid. Our future endeavors will also include testing this methodology for estimating CO_2 emissions for other years and also to include the CO_2 emissions from gas flaring [21] observed in DMSP nighttime lights and electric power utilities based on locations and emission estimates from organizations such as CARMA.

References

1. Weeks, J.R. *Population: An Introduction to Concepts and Issues*, 9th ed.; Wadsworth/Thomson Learning: Belmont, CA, USA, 2005.

2. Population Reference Bureau. *2009 World Population Data Sheet*; Population Reference Bureau: Washington, DC, USA, 2009.
3. IPCC. Summary for Policymakers. In *Climate Change 2007: The Physical Science Basis. Contribution of Working Group I to the Fourth Assessment Report of the Intergovernmental Panel on Climate Change*; Solomon, S., Qin, D., Manning, M., Chen, Z., Marquis, M., Averyt, K.B., Tignor, M., Miller, H.L., Eds.; Cambridge University Press: Cambridge, UK; New York, NY, USA, 2007.
4. Gurney, K.R. Research needs for process-driven, finely resolved fossil fuel carbon dioxide emissions. *EOS Trans.* **2007**, *88*, 542–543.
5. Raupach, M.R.; Rayner, P.J.; Paget, M. Regional variations in spatial structure of nightlights, population density and fossil fuel CO_2 emissions. *Energy Policy* **2009**, 1–9.
6. Gurney, K.R.; Law, R.M.; Denning, A.S.; Rayner, P.J.; Baker, D.; Bousquet, P.; Bruhwiler, L.; Chen, Y.H.; Ciais, P.; Fan, S.; Fung, I.Y.; Gloor, M.; Heimann, M.; Higuchi, K.; John, J.; Maki, T.; Maksyutov, S.; Masarie, K.; Peylin, P.; Prather, M.; Pak, B.C.; Randerson, J.; Sarmiento, J.L.; Taguchi, S.; Takahashi, T.; Yuen, C.W. Towards robust regional estimates of CO_2 sources and sinks using atmospheric transport models. *Nature* **2002**, *415*, 626–630.
7. Gurney, K.R.; Law, R.M.; Denning, A.S.; Rayner, P.J.; Baker, D.; Bousquet, P.; Bruhwiler, L.; Chen, Y.H.; Ciais, P.; Fan, S.M.; Fung, I.Y.; Gloor, M.; Heimann, M.; Higuchi, K.; John, J.; Kowalczyk, E.; Maki, T.; Maksyutov, S.; Peylin, P.; Prather, M.; Pak, B.C.; Sarmiento, J.L.; Taguchi, S.; Takahashi, T.; Yuen, C.W. TransCom 3 CO_2 inversion intercomparison: 1. annual mean control results and sensitivity to transport and prior flux information. *Tellus Ser. B* **2003**, *55*, 555–579.
8. Rayner, P.J.; Scholze, M.; Knorr, W.; Kaminski, T.; Giering, R.; Widmann, H. Two decades of terrestrial carbon fluxes from a carbon cycle data assimilation system (CCDAS). *Global Biogeochem. Cycles* **2005**, *19*.
9. Stephens, B.B.; Gurney, K.R.; Tans, P.P.; Peters, W.; Bruhwiler, L.; Ciais, P.; Ramonet, M.; Sweeney, C.; Bousquet, P.; Nakazawa, T.; Aoki, S.; Machida, T.; Inoue, G.; Vinnichenko, N.; Lloyd, J.; Jordan, A.; Heimann, M.; Shibistova, O.; Langenfelds, R.L.; Steele, L.P.; Francey, R.J.; Denning, A.S. Weak northern and strong tropical land carbon uptake from vertical profiles of atmospheric CO_2. *Science* **2007**, *316*, 1732–1735.
10. Andres, R.J.; Marland, G.; Fung, I.; Matthews, E. A 1° × 1° distribution of carbon dioxide emissions from fossil fuel consumption and cement manufacture, 1950–1990. *Global Biogeochem. Cycles* **1996**, *10*, 419–429.
11. Brenkert, A.L. Carbon dioxide emission estimates from fossil-fuel burning, hydraulic cement production, and gas flaring for 1995 on a one degree grid cell basis, 1998; Available online: http://cdiac.esd.ornl.gov/ndps/ndp058a.html (accessed on 7 December 2010).
12. Olivier, J.G.; Aardenne, J.A.V.; Dentener, F.J.; Pagliari, V.; Ganzeveld, L.N.; Peters, J.A.H.W. Recent trends in global greenhouse gas emissions: Regional trends 1970-2000 and spatial distribution of key sources. *J. Integr. Environ. Sci.* **2005**, *2*, 81–99.
13. Oda, T.; Maksyutov, S. A very high-resolution global fossil fuel CO_2 emission inventory derived using a point source database and satellite-observed nighttime lights, 1980–2007. *Atmos. Chem. Phys.* **2010**, in press.

14. Elvidge, C.D.; Baugh, K.E.; Kihn, E.A.; Koehl, H.W.; Davis, E.R.; Davis, C.W. Relation between satellite observed visible near-infrared emissions, population, economic activity and power consumption, *Int. J. Remote Sens.* **1997**, *18*, 1373–1379.
15. Doll, C.N.H.; Muller, J-P.; Elvidge, C.D. Nighttime imagery as a tool for global mapping of socioeconomic parameters and greenhouse gas emissions, *Ambio* **2000**, *29*, 157–162.
16. Doll, C.N.H. *CIESIN Thematic Guide to Night-Time Light Remote Sensing and its Applications*; Center for International Earth Science Information Network: Palisades, NY, USA, 2008.
17. Rayner, P.J.; Raupach, M.R.; Paget, M.; Peylin, P.; Koffi, E. A new global gridded dataset of CO_2 emissions from fossil fuel combustion: 1: Methodology and evaluation. *J. Geophys. Res.* **2009**, submitted.
18. Gurney, K.R.; Mendoza, D.; Zhou, Y.; Fischer, M.; Miller, C.; Geethakumar, S.; de la Rue du, Can. The Vulcan project: High resolution fossil fuel combustion CO_2 emissions fluxes for the United States. *Environ. Sci. Technol.* **2009**, *43*, 5535–5541.
19. Elvidge, C.D.; Erwin, E.H.; Baugh, K.E.; Ziskin, D.; Tuttle, B.T.; Ghosh, T.; Sutton, P.C. Overview of DMSP nighttime lights and future possibilities. In Proceedings of the 7th International Urban Remote Sensing Conference, Shanghai, China, 20–22 May 2009.
20. Elvidge C.D.; Baugh, K.E.; Dietz, J.B.; Bland, T.; Sutton, P.C.; Kroehl, H.W. Radiance calibration of DMSP-OLS low-light imaging data of human settlements. *Remote Sens. Environ.* **1999**, *68*, 77–88.
21. Elvidge, C.D.; Ziskin, D.; Baugh, K.E.; Tuttle, B.T.; Ghosh, T.; Pack, D.W.; Erwin, E.H.; Zhizhin, M. A fifteen year record of global natural gas flaring derived from satellite data. *Energies* **2009**, *2*, 595–622.
22. *LandScan Global Population Database*; Oak Ridge National Laboratory: Oak Ridge, TN, USA, 2000.
23. United Nations. Millennium Development Goal Indicators. Carbon Dioxide Emissions Data; Carbon Dioxide Information Analysis Center; United Nations Framework Convention on Climate Change, 2000; Available online: http://millenniumindicators.un.org/unsd/mdg/Data.aspx (accessed on June 8 2010).
24. Environmental Protection Agency. State Energy CO_2 Emissions, 2000. Available online: http://www.epa.gov/climatechange/emissions/state_energyco2inv.html (accessed on June 8 2010).
25. Carbon Monitoring for Action, 2000; Available online: http://carma.org/dig (accessed on 8 June 2010).
26. Elvidge, C.D.; Baugh, K.E.; Sutton, P.C.; Bhaduri, B.; Tuttle, B.T.; Ghosh, T.; Ziskin, D.; Erwin, E.H. Who's in the dark: satellite based estimates of electrification rates. In *Urban Remote Sensing: Monitoring, Synthesis and Modeling in the Urban Environment*; Yang, X., Ed.; Wiley-Blackwell: Chichester, UK, in press.
27. McLendon, R. *Urban or Rural: Which is More Energy Efficient?*; Available online: http://www.mnn.com/earth-matters/translating-uncle-sam/stories/urban-or-rural-which-is-more-energy-efficient (accessed on 20 November 2010).
28. Elvidge, C.D.; Cinzano, P.; Pettit, D.R.; Arvesen, J.; Sutton, P.; Small, C.; Nemani, R.; Longcore, T.; Rich, C.; Safran, J.; Weeks, J.; Ebener, S. The Nightsat mission concept. *Int. J. Remote Sens.* **2007**, *28*, 2645–2670.

29. Elvidge C.D.; Keith D.M.; Tuttle B.T.; Baugh K.E. Spectral identification of lighting type and character. *Sensors* **2010**, *10*, 3961–3988.

© 2010 by the authors; licensee MDPI, Basel, Switzerland. This article is an open access article distributed under the terms and conditions of the Creative Commons Attribution license (http://creativecommons.org/licenses/by/3.0/).